Optics Letters

Resetting directional couplers for high-fidelity quantum photonic integrated chips

Feng Yu,[1] Zhen-Nan Tian,[1,5] Simone Piacentini,[2,3] Xiao-Yan Li,[1] Qi-Dai Chen,[1] Roberto Osellame,[2,3] and Hong-Bo Sun[1,4,6]

[1]State Key Laboratory of Integrated Optoelectronics, College of Electronic Science and Engineering, Jilin University, Changchun 130012, China
[2]Dipartimento di Fisica-Politecnico di Milano, piazza L. da Vinci 32, 20133 Milano, Italy
[3]Istituto di Fotonica e Nanotecnologie-Consiglio Nazionale delle Ricerche (IFN-CNR), piazza L. da Vinci 32, 20133 Milano, Italy
[4]State Key Laboratory of Precision Measurement Technology and Instruments, Department of Precision Instrument, Tsinghua University, Haidian, Beijing 100084, China
[5]e-mail: zhennan_tian@jlu.edu.cn
[6]e-mail: hbsun@tsinghua.edu.cn

Received 2 August 2021; revised 17 September 2021; accepted 21 September 2021; posted 22 September 2021 (Doc. ID 439178); published 11 October 2021

In this Letter, we propose a fabrication technique based on femtosecond laser secondary direct writing (FsLSDW) that allows us to statically reset the beam-splitting ratio of directional couplers. By modifying the interaction region with a second inscription, the coupling coefficient of the reconstructed devices can be indeed changed continuously within the range of 0.49–2.1 rad/mm, thus enabling a complete tunability of the reconstructed splitting ratio from zero to full power transfer between the waveguides. This powerful reconstruction capability facilitates the arbitrary reset of an imperfect device, from any initial splitting ratio to the correct one. In the future, such static control method could potentially solve the fabrication error problem in the manufacturing of high-fidelity large-scale integrated photonic quantum chips.

https://doi.org/10.1364/OL.439178

The directional coupler (DC), an integrated device capable of performing power exchange between two adjacent waveguides via evanescent coupling [1,2], is a vital component of quantum photonic integrated chips (QPICs) [3–5]. Recently, numerous promising technologies have been proposed for the fabrication of DCs on chips [6–9]. The femtosecond laser direct writing (FsLDW) technology [10–12] plays an important role in manufacturing QPICs, being a maskless, real three-dimensional (3D) technique, which provides high flexibility and having a fast production capability [13–15]. The FsLDW-based chips made up of multiple DCs demonstrate a thrilling ability to process information in quantum computing and simulation [1,16,17]. This excellent capability of the QPIC [16–18] is highly dependent on the splitting ratio accuracy of the DCs that form them [19,20]. However, the DCs fabricated by any technology are affected by inevitable fabrication errors, owing to the limitations of processing equipment and environment [21,22]. For complex devices made of several DCs, such imperfections would add up, thus causing a degradation of the chip performance or loss of operation in the worst case.

To solve this issue, a Mach–Zehnder interferometer with a phase control could replace a passive DC, acting in fact as a two-port device with a tunable splitting ratio. In this respect, several control schemes have been proposed [23–25]. Thus, in 2019, a successful implementation of a reconfigurable multifunctional lithium niobate photonic integrated chip, based on the electro-optic effect of crystals, was presented [23]. In 2020, a low thermal crosstalk and low-operating-voltage thermal-phase shifter, based on the thermo-optic effect in glass, were demonstrated [24]. These active control methods have significantly improved the fidelity and chip dynamic operations, but they have also increased the device complexity and caused additional power consumption. However, an active reconfiguration of circuit properties is not required, but only a compensation for the fabrication tolerances, passive control schemes, based on multiple laser scans, are very interesting as they can achieve the goal without introducing any further elements into the circuit layout [26,27]. In 2020, adjustment of the propagation constant of a waveguide was demonstrated using multi-scanning, which makes the beam-splitting ratio (BSR) of DCs change for about 0.3 [25]. However, in this case, the maximum power transfer of DCs could not reach 100% because of the detuning between the coupled waveguides, which poses a challenge in achieving a full-period control. Therefore, it is necessary to develop a new control method with high adjustment capability without introducing additional electrodes to fabricate high-fidelity QPICs.

Here, we propose a static control method to reset the BSR of the DCs via reconstructing the coupling spacing using the FsLSDW. The coupling coefficient of the reconstructed DC can be continuously changed in the range from 0.49 to 2.1 rad/mm, with a stable maximum achievable power transfer and initial phase. Owing to this powerful reconstruction ability, imperfect devices with the initial BSR of 52.3:47.7 and 10.5:89.5 can be altered to BSRs of 50.2:49.8 and 0.3:99.7, respectively, which are very close to the commonly used splitting ratios of 50:50 and 0:100. Furthermore, this study demonstrates that

the reset of imperfect devices can achieve the full range of BSR, irrespectively of its initial value, by adjusting the coupling distance between the two waveguides. This static control method is advantageous as it is a simple process, presenting no thermal crosstalk and no extra power consumption. Furthermore, it is suitable for resetting the 3D device and thus overcoming the problem of the QPICs manufacturing tolerance.

According to the coupled mode theory (CMT) [28,29], the BSR of DCs is closely related to the coupling coefficient (κ), coupling length (L), and propagation constant (β) of waveguides [30,31]. Assuming that light is injected in only one input port of the DC, the BSR satisfies the following equation [25,32]:

$$\mathrm{BSR} = \frac{P_2}{P_1 + P_2} = \delta^2 \times \sin^2\left(\frac{\kappa}{\delta} \times L + \varphi_0\right), \tag{1}$$

where

$$\delta^2 = \frac{4\kappa^2}{4\kappa^2 + \Delta\beta^2}. \tag{2}$$

$\Delta\beta = |\beta_1 - \beta_2|$ is the difference between the two waveguide propagation constants β_1 and β_2, and P_1 (P_2) denotes the output power of Waveguide 1 (Waveguide 2). φ_0 is the initial phase caused by the coupling occurring in the bending regions in DCs. Theoretically, the change of any of these parameters, i.e., κ, L, and β, can modify the BSR of the DCs. However, in the photonic circuit to be repaired, the initial devices fabricated by the first laser direct writing have a fixed size, so it would be difficult to change L. In addition, Eqs. (1) and (2) show that when $\Delta\beta \neq 0, \delta < 1$, and therefore $\mathrm{BSR_{MAX}} < 1$. This indicates that the input light could not be completely transferred from one waveguide to the other, thus making it difficult to realize a DC with a BSR of 0:100. In conclusion, it is observed that the best parameter to act on in an already existing DC is the coupling coefficient, since its modification would enable a full BSR tunability without requiring a change in size of the device. According to the CMT, the coupling coefficient of DCs sisfies the following relationship [28,32]:

$$\kappa = \kappa_1 \mathrm{e}^{-\frac{d}{d_1}}. \tag{3}$$

Here, κ_1 and d_1 are suitable constants, d is the distance between the centers of two coupling waveguides in the coupling region. According to Eqs. (1)–(3), it is feasible to reset the BSR of the DCs by controlling the coupling distance between the two waveguides in the interaction region.

The proposed method to reconstruct the coupling distance using the FsLSDW is shown in Fig. 1(a). The gray lines represent the initial waveguides (IWGs) fabricated using the FsLDW for the first time. The initial directional couplers (IDCs) composed of IWGs have a fixed coupling length, L_0, and a fixed coupling distance, d_0. Two additional waveguides are inscribed in the coupling region using FsLSDW to change d_0. The combined waveguide (CWG) obtained by inscribing the secondary waveguide (SWG) with FsLSDW close to the IWG has a new cross-section size and geometric center. As shown in Figs. 1(b)–1(d), when the SWGs are on the inner side of the coupling regions, the geometric centers of the two CWGs get closer to each other, and the d_0 is reduced to d_{WG}. Conversely, when the SWGs are outside the coupling regions, the geometric centers of the two waveguides get farther, and the d_0 is increased to d'_{WG}. Therefore, the reconstructed directional couplers

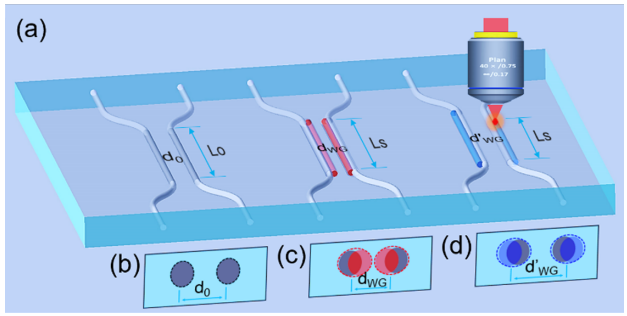

Fig. 1. Schematic diagram of the reconstruction of the DCs coupling distance by FsLSDW. (a) Initial DCs and reconstructed directional couplers (RDCs), where L_0 and L_S are the lengths of IWGs and SWGs in the coupling regions, respectively. (b)–(d) are the cross-sectional diagrams of the two waveguides in the coupling regions of DCs.

(RDCs) composed of CWGs have a new coupling spacing d_{WG} or d'_{WG}.

In the experiment, the femtosecond laser pulse (pulse width of 290 fs, wavelength of 1029 nm) from the amplifier (Light Conversion, Carbide 5 W) was focused 170 μm below the surface of boroaluminosilicate glass (Corning, Eagle 2000) using a dry objective lens (NA = 0.75, 40×) to prepare IWGs and SWGs with the same parameters. The repetition rate, single-pulse energy, and scanning speed used were 1 MHz, 0.24 μJ, and 40 mm/s, respectively. As shown in Figs. 2(a) and 2(c), the distance d_0 between the two IWGs in the coupling region is always 8 μm. Furthermore, as shown in Figs. 2(a1)–2(a3), when the SWGs are inscribed on the inner side of the coupling region, the variation of the distance between the IWGs and SWGs is $2\Delta d_i$, with $\Delta d_i < 0$. The transverse dimension of the CWGs increases gradually with an increase in $|2\Delta d_i|$, while the distance between the geometric centers of the two CWGs ($d_{\mathrm{WG}} = d_0 + 2\Delta d_i$) decreases gradually.

As shown in Figs. 2(c1)–2(c3), when the SWGs are outside the coupling region, the variation of the distance between the IWGs and the SWGs is $2\Delta d'_i$, with $\Delta d'_I > 0$. The distance between the geometric centers of the two CWGs ($d'_{\mathrm{WG}} = d_0 + 2\Delta d'_i$) also increases gradually due to the increase in $|2\Delta d'_i|$. The overlap integral of the CWGs mode fields in the coupling region varies with the geometric center of CWGs since the mode field and the geometric centers of the CWGs nearly coincide. In particular, it increases gradually as the center distance of the CWGs decreases, as shown in Figs. 2(b1)–2(b3), while the opposite occurs when the distance increases, as shown in Figs. 2(c1)–2(c3). For preserving the single-mode operation of CWGs, $|2\Delta d_i|$ ($|2\Delta d'_i|$) can vary within the range of 0–3 μm. Therefore, the reconstructed coupling spacing is adjustable within the range of 5–11 μm (initial coupling spacing $d_0 = 8$ μm), and the overlap integral of the two waveguides in the coupling region is adjustable within the range of 24.4%–56.7% (initial overlap 40.2%).

The coupling coefficient of the DC with the reconstructed coupling distance can thus be reset within a large range, while the maximum achievable transmittance and initial phase remain relatively unchanged. In the experiment, the transmission and BSR of the devices were measured using the 808 nm continuous laser (CNI, MDL-III-808L). The transmission of the IDCs and RDCs satisfies Eq. (1), as shown in Fig. 3(a).

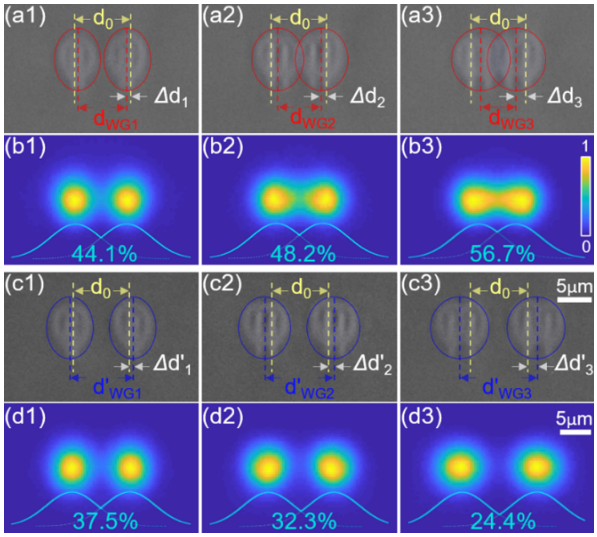

Fig. 2. Experimental diagram of the reconstruction of the DCs coupling distance by FsLSDW. (a1)–(a3) and (b1)–(b3) cross-sectional micrographs and mode field distributions of the two CWGs when SWGs are inside the coupling region. (c1)–(c3) and (d1)–(d3) are cross-sectional micrographs and mode field distributions of the two CWGs when SWGs are outside the coupling region. d_0 is the initial coupling distance between the two IWGs. $2\Delta d_1$ ($2\Delta d_1'$), $2\Delta d_2$ ($2\Delta d_2'$), and $2\Delta d_3$ ($2\Delta d_3'$) represent the distances between SWG and IWG, which are -1 μm (1 μm), -2 μm (2 μm), and -3 μm (3 μm), respectively. The geometric center of CWGs can be approximately considered to be the average of the geometric centers of IWGs and SWGs, so the distance between SWGs and CWGs is Δd_i. Calculated overlap percentages between the mode field distributions are provided in (b1)–(b3) and (d1)–(d3).

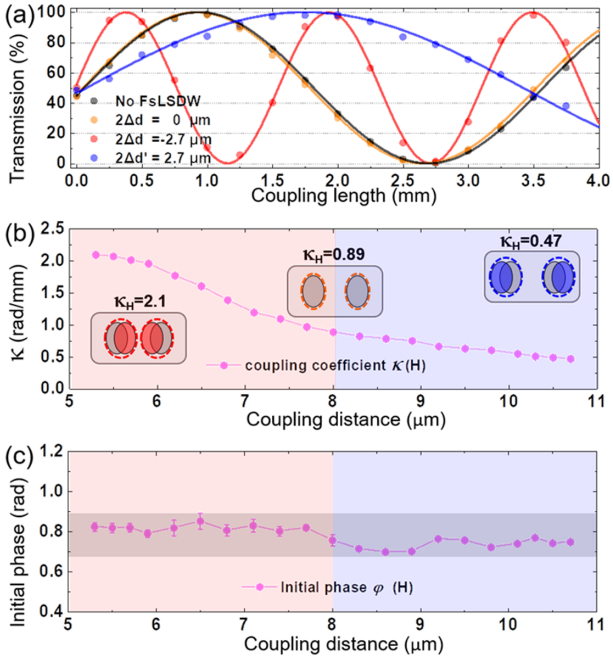

Fig. 3. Variation trend of maximum transmission, coupling coefficient, and initial phase with coupling distance in RDCs. (a) When $L_0 = L_S$, the transmission of IDCs and RDCs changes with the length of CWGs. (b) and (c) are curves of the coupling coefficient and initial phase varying with reconstructed coupling distances, respectively.

When $2\Delta d_i = 0$ μm, the oscillation period and coupling coefficient of the RDCs and IDCs are almost identical. However, the oscillation periods and coupling coefficients vary significantly with the change in $2\Delta d_i$. The maximum transmittance of all the DCs is close to 100% because the two waveguides in the coupling region have identical propagation constants. The coupling coefficient variation trend of RDCs with the reconstructed coupling distance is in agreement with Eq. (3), as shown in Fig. 3(b). When the coupling distance increases from 5 to 11 μm (initial coupling distance $d_0 = 8$ μm), the coupling coefficient decreases from 2.1 to 0.47 rad/mm (initial coupling coefficient $\kappa_0 = 0.89$ rad/mm). Since only the coupling regions of the DCs are reconstructed, the initial phase generated by the coupling effect in the bending regions does not change with the reconstruction of the coupling distance. When the coupling length is 0 mm, all the curves meet at almost the same point, and Trans. ≈ 0.45, as shown in Fig. 3(a). It can be seen from Eq. (1), that when Trans. ≈ 0.45, $\delta = 1$, and $L = 0$ mm, a $\varphi_0 \approx 0.78$ rad is observed. As shown in Fig. 3(c), the initial phase is almost stable at 0.78 rad for different coupling distances, and the standard deviation is only 4.6%. In addition, the writing of the SWGs causes the mode size mismatch of the IWGs and CWGs, which increases the overall RDCs loss. When the distance between SWG and IWG gradually increases from 0 to 2.7 μm, the overall RDC loss increases gradually from 1.29 to 2.23 dB. The overall loss of IDC is about 1.24 dB.

Two reconstruction strategies have been proposed to realize the reset of imperfect devices by benefitting from the advantages of the wide range of coupling coefficient adjustments. In the first one, the SWGs and IWGs in the coupling regions have identical lengths ($L_0 = L_S$), and the coupling distance of the two CWGs varies with the position of the SWGs, as shown in Fig. 4(a). According to the gray curve in Fig. 3(a), when $L_0 = 1.83$ mm ($L_0 = 2.73$ mm), the theoretical value of the initial BSR of DC should be 50:50 (0:100). However, the actual value of the initial BSR is 52.3:47.7 (10.5:89.5) owing to the fabrication error, as shown at point A0 (B0) in Fig. 4(c). The process of resetting the BSR with FsLSDW is demonstrated, because the device is repaired to a near ideal BSR of 50.2:49.8 (0.3:99.7), while the reconstructed coupling spacing is 7.95 μm (8.75 μm), as shown in point A1 (B1) in Fig. 4(c). The solid and dashed lines in Fig. 4(c) indicate that the initial BSR of the devices can be reset to any final BSR when the coupling spacing is varied from 6 to 10 μm. In addition to the full range reset strategy mentioned above, we also propose another strategy that can realize multiple reset to achieve better repair results. When the reconstructed distance is fixed, multiple resets of BSR of DCs can be realized by extending the length of the secondary waveguides several times ($0 \le Ls \le L_0$), as shown in Fig. 4(b). Specifically, when the reconstructed distance is 1 μm (-1 μm), the relationship between the BSR and length of SWGs is shown by the blue (red) line in Fig. 4(d). Here, C0 represents the initial BSR of the devices, and C1–C4 represent several relevant values that can be targeted in the process of resetting the BSR of the devices. These two methods of resetting the BSR of directional coupler provide the possibility to solve the problem of fabrication errors.

In summary, this Letter proposed a static control scheme to reset the BSR of DCs based on the reconstruction of coupling spacing by FsLSDW to solve the problem of fabrication error in the process of photonic quantum chip manufacturing. In this study, the DCs were fabricated with an initial coupling distance of 8 μm in the Corning Eagle 2000 using a femtosecond laser. We showed that the coupling distance can vary from 5 to

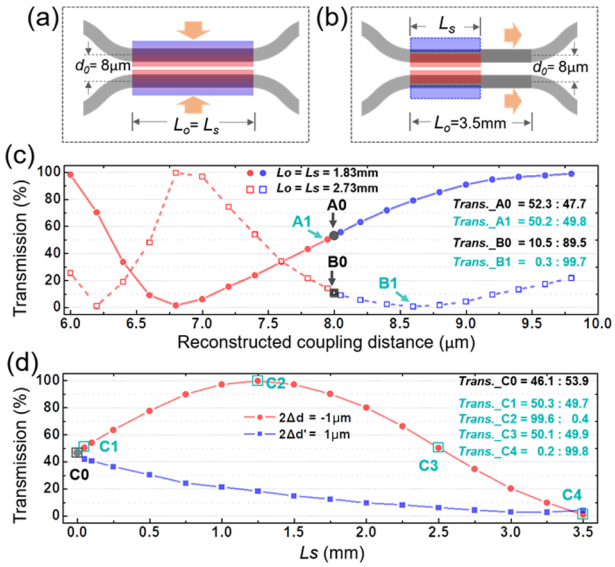

Fig. 4. Repair and reset of imperfect devices. (a) The schematic diagram of BSR resetting by fixing the SWG length and changing the coupling spacing. (b) The schematic diagram of BSR resetting by fixing the reconstructed distance and changing the length of SWGs. (c) The relationship between the reset BSR and the reconstructed coupling spacing. (d) The correlation between the reset BSR and the length of SWGs.

11 μm by reconstructing two IWGs in the coupling region. The coupling coefficient of a reconstructed device can be changed continuously within the range of 0.49–2.1 rad/mm (the initial coupling coefficient is 0.89 rad/mm), while the maximum transmission and initial phase remain almost unchanged. The error repair of the non-ideal device is demonstrated by employing the above control scheme, and the initial BSR of the device is reset to any final BSR several times. This static control method is advantageous as it involves a simple process, without thermal cross talk, and without extra power consumption, and it can be applied to the control of 3D photonic devices. This method can potentially solve the fabrication error of photonic quantum devices. In addition, the imperfect chip can be repaired in real time by combining this static control method with some photonic integrated chip detection technology, and it can be used to fabricate a high-fidelity 3D large-scale photonic quantum integrated chip.

Funding. National Key Research and Development Program of China (2016YFA0301700); National Natural Science Foundation of China (61590930, 61805098, 61825502, 61827826).

Disclosures. The authors declare no conflict of interest.

Data Availability. Data underlying the results presented in this paper are not publicly available at this time but may be obtained from the authors upon reasonable request.

REFERENCES

1. L. Sansoni, F. Sciarrino, G. Vallone, P. Mataloni, A. Crespi, R. Ramponi, and R. Osellame, Phys. Rev. Lett. **108**, 010502 (2012).
2. F. Yu, L. C. Wang, Y. Chen, Q. D. Chen, Z. N. Tian, X. F. Ren, and H. B. Sun, J. Lightwave Technol. **39**, 1451 (2021).
3. J. Liu, Q. H. Wu, X. B. Sui, Q. Chen, G. H. Gu, L. P. Wang, and S. C. Li, PhotoniX **2**, 5 (2021).
4. E. Goi, Q. M. Zhang, X. Chen, H. T. Luan, and M. Gu, PhotoniX **1**, 3 (2020).
5. Q. Zhang, M. Li, Y. Chen, X. F. Ren, R. Osellame, Q. H. Gong, and Y. Li, Opt. Mater. Express **9**, 2318 (2019).
6. K. H. Luo, S. Brauner, C. Eigner, P. R. Sharapova, R. Ricken, T. Meier, H. Herrmann, and C. Silberhorn, Sci. Adv. **5**, eaat1451 (2019).
7. L. T. Feng, M. Zhang, Z. Y. Zhou, M. Li, X. Xiong, L. Yu, B. S. Shi, G. P. Guo, D. X. Dai, X. F. Ren, and G. C. Guo, Nat. Commun. **7**, 11985 (2016).
8. C. R. Ocier, C. A. Richards, D. A. Bacon-Brown, Q. Ding, R. Kumar, T. J. Garcia, J. van de Groep, J. H. Song, A. J. Cyphersmith, A. Rhode, A. N. Perry, A. J. Littlefield, J. L. Zhu, D. J. Xie, H. B. Gao, J. F. Messinger, M. L. Brongersma, K. C. Toussaint, Jr., L. L. Goddard, and P. V. Braun, Light Sci. Appl. **9**, 196 (2020).
9. S. Chen, M. P. Zhuo, X. D. Wang, G. Q. Wei, and L. S. Liao, PhotoniX **2**, 2 (2021).
10. X. Q. Liu, Q. D. Chen, K. M. Guan, Z. C. Ma, Y. H. Yu, Q. K. Li, Z. N. Tian, and H. B. Sun, Laser Photon. Rev. **11**, 1600115 (2017).
11. Z. Z. Li, L. Wang, H. Fan, Y. H. Yu, H. B. Sun, S. Juodkazis, and Q. D. Chen, Light Sci. Appl. **9**, 41 (2020).
12. M. D. Qian, Y. L. Sun, Z. Y. Hu, X. F. Fang, J. L. Zhu, X. D. Fan, Q. Liao, C. F. Wu, and H. B. Sun, Mater. Horiz. **7**, 1782 (2020).
13. Z. S. Hou, X. Xiong, J. J. Cao, Q. D. Chen, Z. N. Tian, X. F. Ren, and H. B. Sun, Adv. Opt. Mater. **7**, 1900129 (2019).
14. F. D. Marquis, J. Gargiulo, E. G. Lopez, B. Jang, T. Kroh, C. Mueller, M. Ziegler, S. A. Maier, H. Kuebler, M. A. Schmidt, and O. Benson, Light Sci. Appl. **10**, 114 (2021).
15. A. Cerjan, M. H. Wang, S. Huang, K. P. Chen, and M. C. Rechtsman, Light Sci. Appl. **9**, 178 (2020).
16. A. Crespi, R. Osellame, R. Ramponi, V. Giovannetti, R. Fazio, L. Sansoni, F. D. Nicola, F. Sciarrino, and P. Mataloni, Nat. Photonics **7**, 322 (2013).
17. H. Tang, X. F. Lin, Z. Feng, J. Y. Chen, J. Gao, K. Sun, C. Y. Wang, P. C. Lai, X. Y. Xu, Y. Wang, L. F. Qiao, A. L. Yang, and X. M. Jin, Sci. Adv. **4**, eaat3174 (2018).
18. L. Wang, G. Dai, L. G. Deng, and H. Z. Zhong, Sci. China Mater. **63**, 1382 (2020).
19. D. A. B. Miller, Optica **2**, 747 (2015).
20. J. Mower, N. C. Harris, G. R. Steinbrecher, Y. Lahini, and D. Englund, Phys. Rev. A **92**, 032322 (2015).
21. A. Crespi, R. Ramponi, R. Osellame, L. Sansoni, I. Bongioanni, F. Sciarrino, G. Vallone, and P. Mataloni, Nat. Commun. **2**, 566 (2011).
22. I. V. Dyakonov, M. Y. Saygin, I. V. Kondratyev, A. A. Kalinkin, S. S. Straupe, and S. P. Kulik, Opt. Lett. **42**, 4231 (2017).
23. R. B. Wu, J. T. Lin, M. Wang, Z. W. Fang, W. Chu, J. H. Zhang, J. X. Zhou, and Y. Cheng, Opt. Lett. **44**, 4698 (2019).
24. F. Ceccarelli, S. Atzeni, C. Pentangelo, F. Pellegatta, A. Crespi, and R. Osellame, Laser Photon. Rev. **14**, 2000024 (2020).
25. T. Will, J. Guan, P. S. Salter, and M. J. Booth, Opt. Express **28**, 28006 (2020).
26. R. Heilmann, C. Greganti, M. Graefe, S. Nolte, P. Walther, and A. Szameit, Appl. Opt. **57**, 377 (2018).
27. Z. M. Liu, Y. Liao, Z. H. Wang, Z. H. Zhang, Z. X. Liu, L. L. Qiao, and Y. Cheng, Materials **11**, 1926 (2018).
28. W. P. Huang, J. Opt. Soc. Am. A **11**, 963 (1994).
29. A. Hardy and W. Streifer, J. Lightwave Technol. **3**, 1135 (1985).
30. A. Szameit, F. Dreisow, T. Pertsch, S. Nolte, and A. Tuennermann, Opt. Express **15**, 1579 (2007).
31. K. Minoshima, A. M. Kowalevicz, E. P. Ippen, and J. G. Fujimoto, Opt. Express **10**, 645 (2002).
32. I. Pitsios, F. Samara, G. Corrielli, A. Crespi, and R. Osellame, Sci. Rep. **7**, 11342 (2017).